Design, construction and performance evaluation of an almond kernel extraction machine

Samy Marey[1,4*], A. M. Drees[2], M. M. Ibrahim[3], M. A. Aboegela[4]

(1. *Sciences*, *Technology and Innovation Unit, King Saud University*; *P.O. Box*: *2454*; *Riyadh 11451*; *Saudi Arabia*;
2. *Department of Agricultural Engineering*; *College of Agriculture*, *Al Azher University*, *Egypt*;
3. *Department of Agricultural Engineering*, *College of Agriculture*, *Cairo University*, *Egypt*;
4. *Agricultural Engineering Research Institute* (*AENRI*), *Agricultural Research Centre*, *P.O Box 256 Dokki*, *Giza*, *Egypt*)

Abstract: A low-cost almond (Prunus *dulcis*) kernel extraction machine was locally designed, manufactured and evaluated. Kernel extraction by the machine was conducted by first crushing the nut, and then separating seeds from a shell. The performance of the developed machine was evaluated in terms of machine productivity, cracking efficiency, kernel breakage and specific energy requirements. The evaluation was conducted at roller speeds (ranging from 0.5 to 1 m s^{-1}), rollers clearance (ranging from 14 to 25 mm) and two different roller casing materials (rubber and metal mesh). Results revealed that the increase of the roller speed was found to increase the machine productivity. However, it caused a decrease in the kernel breakage, cracking efficiency, energy requirements and the extraction cost. At all levels of roller speeds and both casing materials, the clearance between rollers of 16 mm resulted in lowest values of energy requirement, extraction cost and highest values of machine productivity. On the other hand, the clearance between rollers of 14 mm resulted in the maximum values of cracking efficiency. The use of rubber casing was found to increase the machine productivity, cracking efficiency and decrease the kernel breakage, energy requirements and extraction cost.

Keywords: almonds, machine design, kernel extraction, cracking efficiency

Citation: Marey, S., A. M. Drees, M. M. Ibrahim, and M. A. Aboegela. 2017. Design, construction and performance evaluation of an almond kernel extraction machine. Agricultural Engineering International: CIGR Journal, 19(4): 133–144.

1 Introduction

Almond (Prunus *dulcis*) is a perennial plant grown in cold temperate-regions. The kernel has an important source of energy (6 kcal g^{-1}), protein (15.64%) and the oil content ranges from 35.27% to 40% (Aydin, 2003). Approximately 98% of the sold almonds is shelled either naturally with retaining the brown skin or blanched with removing the skins. Almonds can be eaten as a dessert nut either dry roasted or roasted in almond oil, then salted and seasoned. They are also used for baking, confectionery, cereal, dairy or snack formulations. Processing may produce blanched completely, slivered, meal, diced, split, sliced or flaked almonds; almond butter is a recent development (Rosengarten, 1984; Paramount Farms Almonds, 1991). Almond shell is used in many industrial applications (Estevinho et al., 2006; Ahmedna et al., 2004; Mitchell et al., 2003) and hydroponic as well (Lao and Jimenez, 2004). The cracking process is the most critical and delicate step for achieving high-quality kernels. The traditional method for cracking almond (manually) is labour intensive, slow and tedious. The mechanical properties of the nuts are a pre-requisite for the design and development of a cracking machine (Guzel et al., 1999; Khazaei, 2008). Ghafari et al. (2011) stated that the walnut extraction quality depended on the shell moisture content, shell thickness, nut size and loading positions in nuts. However, Eric et al. (2009) stated that the dominant physical properties that influenced nut cracking are rotor speed, nut size, nut variety and moisture content. The cracking position had an important effect on extracting the kernels. Khazaei et al (2002) found that the almond size and loading direction has a

Received date: 2017-01-01 **Accepted date:** 2017-02-28

* **Corresponding author: Samy Marey,** Associate professor. 0096592775764 Sciences, Technology and Innovation Unit, King Saud University; P.O. Box: 2454; Riyadh 11451; Saudi Arabia. Email: samyeg2005@yahoo.com.

significant effect on cracking force, absorbed energy and required power. Altuntas et al. (2010) indicated that the effects of compression along the axis and speed on the rupture force were highly dependent on almond cultivars. Aydin (2002) found that the maximum force required to crack almond nuts was measured when nuts were placed at right angles to the longitudinal axis; whereas the minimum force required to crack nuts occurred when the force was applied along the longitudinal axis. Borghei et al. (2000) have investigated the effect of feeding method and walnuts size on the required cracking force. They found that, the cracking force and strain of walnuts were in the range from 110 to 800 N and from 0.01 to 0.045, respectively at 6% moisture content (wet basis). The study also showed that large sized walnuts required higher cracking force than small ones. Many investigators designed different cracking machines with different cracking mechanisms. Ghafari et al. (2011) designed a walnut cracker and evaluated its performance. Their cracker consists of a hopper fitted with a flow rate control device, a cracking unit, a sorter and power system. The principle of attrition is using a crushing force from a cylinder and helix. Ogunsina (2008) designed machine for cracking dika nut; the nuts is fed by hand in a toggle mechanism comprising of a slider and a fixed block. Fracture mechanism was based on the deformation characteristics of dried dika nuts under uni-axial compression. When actuated, the slider compresses the nutshell to failure along its line of symmetry. Koya (2006) modelled and tested two models for cracking palm nut under repeated load. The models were based on the conservation of energy impacted on the nut by falling weight, the kinetic energy of a moving object and the strain energy required for cracking the nutshell. Ojolo and Ogunsina (2007) developed a roasted cashew nuts machine, its components are the metal casing, feeding tray (i.e., supported by mild steel box), cracking lid, and lever arm. The impact of the lid against the feeding tray cracks nuts. The centrifugal nutcrackers have high productivity; however, the process has quite number of deficiencies, which include breaking of kernels in the course of cracking as well as kernel loss. Therefore, the objective of this study was to develop efficient Almonds cracking machine and evaluate its performance. The proposed design is based on increasing cracking efficiency with minimum kernel breakage.

2 Theoretical approach

A roller cracker's mechanism was used. The assumption that the hopper shaping aids discharge by gravity. A roller cracker consists of two counter-rotating cylinders (rollers) to crack nuts (Figure 1). The gap between the rollers is set slightly smaller than the narrowest dimension of the almond nut. The objective is to crack the nut without damage the kernel. For this reason, almond nuts fed into a particular roller cracker must be pre-sized for that cracker. Based on the comparative analysis of cracking mechanisms and its performance (Wang, 1963; Mohsenin, 1986), the cracking of the almond nut is crisscrossed with veins and will stand a strong tensile force.

The frictional coefficients differ between the almond nut, and a material is obvious upon observation and because of this difference in physical characteristics, it was decided that frictional rollers could accomplish the removal of the almond nut.

Diagrammatic sketch shows the forces acting on an almond nut when it passes between two counter- rotating rollers illustrated in Figure 1.

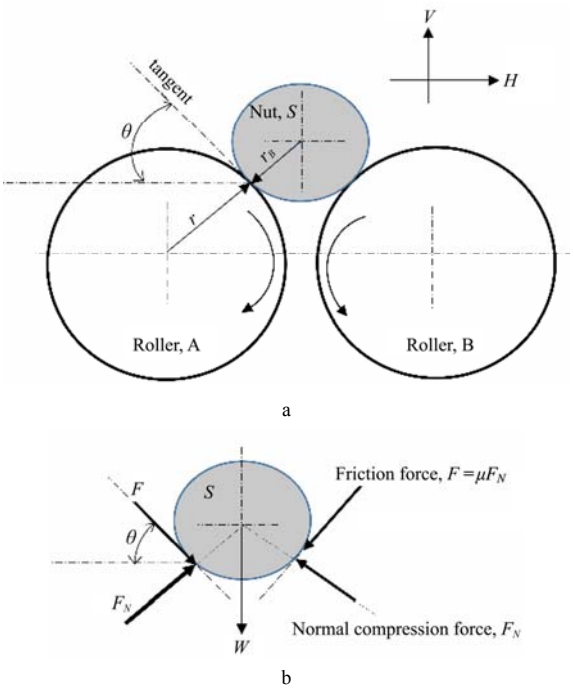

Figure 1 Diagrammatic sketch for the forces acting on a spherical nut during the cracking process

The forces balance in the vertical direction given by:

$$2F\sin\theta + W = 2F_N\cos\theta \quad (1)$$

$$F = \mu F_N \quad (2)$$

where, F (N) is the friction force between the nut and the roller surface; μ is the kinetic friction coefficient between the nut and the roller surfaces; F_N (N) is the normal compression force; W (N) is the weight of the nut; and θ (deg) is the angle between the almond nut S and rollers A and B).

$$2F\left(\sin\theta - \frac{\cos\theta}{\mu}\right) + W = 0 \quad (3)$$

In Figure 1, r is the radius of the roller A or B, r_B is the radius of the spherical nut (S) and h is the distance between two rollers.

$$2F\left(\frac{\cos\theta}{\mu} - \sin\theta\right) = W > 0 \quad (4)$$

Hence,

$$cot\theta > 0 \quad (5)$$

However, based on the diagram in Figure 1, cot θ expressed as follows:

$$cot\theta = \frac{\sqrt{(r+r_B)^2 - (r+\frac{1}{2}h)^2}}{r+\frac{1}{2}h} = \sqrt{\frac{(r+r_B)^2}{(r+\frac{1}{2}h)^2} - 1} \quad (6)$$

Therefore,

$$\sqrt{\frac{(r+r_B)^2}{(r+\frac{1}{2}h)^2} - 1} > \mu \quad (7)$$

In Equation (7), assuming the radius of the almond nut, r_B, is a constant value and the coefficient μ is always positive (depending on the surface condition of rollers), Equation (7) establishes the maximum limit of the roller radius, r.

The horizontal force that induced by the rollers and applied to the almond (F_H, in N) is the summation of two opposite horizontal forces and expressed as follows:

$$F_H = 2(F\cos\theta + F_N\sin\theta) \quad (8)$$

Combining Equations (8), (2), and (1) leads to:

$$F_H = W\frac{\mu cot\theta + 1}{cot\theta - \mu} \quad (9)$$

In Equation (9), F_H (N) is the maximum horizontal force which almond nut can withstand. When the nut is subjected to a horizontal force beyond this value, berries will be crushed. Therefore, the crushing force, $F_{H,\max}$ (N) is defined as follows:

$$F_{H,\max} > W\frac{\mu cot\theta + 1}{cot\theta - \mu} \quad (10)$$

Equation (10) establishes another limit for the radius of the rollers. However, in this instance, the limit is related to $F_{H,\max}$ and W. The significance of this relationship is discussed in the following section.

From Equation (7), it is evident that the surface properties of the material between the almond nut, and the rollers should be carefully selected. It can also be shown that, if the frictional force between the rollers and the almond nut is to be utilized to crack a nut, the frictional coefficients between the rollers' surfaces and the almond nut are important factors. In Table 2, the frictional coefficients between the almond nut and three different surfaces are illustrated.

The normal compression force (F_N) was determined by placing almond nut between two flat surfaces, as illustrated in Figure 2, and gradually increasing the applied force. It was found that the permanent deformation of almond nut occurred between an applied force of 162.11 and 202.15 N in the direction of the nut width axis, (the nut breaks up).

According to Table 2, the thickness of the almond nuts was in the range between 14.12 mm and 16.88 mm. The equivalent radius of the nut, r_B, was considered as the minimum thickness (14.12 mm). To determine the maximum radius of the roller, r, as dictated by Equation (7), the min values of r_B and μ should be selected (r_B = 14.12 mm and μ = 0.625) and substituted in Equation (7). This means that rollers with radii less than 45 mm will satisfy the limiting condition of Equation (7).

2.1 Design Procedure

The main components of the proposed cracking machine are: (i) cracking unit, (ii) rotating shaft and bearings, (iii) power transmission unit, (iv) feeding unit, and (v) main frame and supporting unit. In addition, the power required to operate the machine is the first step to be consider in the design procedures.

2.1.1 The power required for cracking almond nuts

The power required to crack almond nuts (P, in W) was estimated according to Shigley (2015) as follows:

$$P = n_r\, T\omega \quad (11)$$

where, n_r is the number of the rotating rollers (n_r = 2); ω is the angular velocity of the roller, in rad/second, ($\omega = 2\pi N_s/60$), N_s is the roller speed (in rpm); T is the torque (in N m) and is estimated as:

$$T = r F_t \quad (12)$$

In Equation (12), r is the radius of the rotating roller (r = 45 mm) and F_t is the total friction force induced between the roller surface and the loaded nuts during the crashing process (N).

For one nut, the normal compression force (F_N) that is required to crack one almond nut was measured to be 202.15 N (Table 1) and the corresponding friction force (F) is defined by Equation (2). The force, F was estimated based on a friction coefficient (μ = 0.625) between the rubber (i.e., a rubber layer was fixed on the outer surface of the cylinder to perform the cracking drum) and the almond nuts (Table 1); the value of $F=\mu F_N$ is equals to 127 N. The loading rate is defined as the length of the roller (i.e., the cracking cylinder, 300 mm according to Arnold (1964) divided by the width of the nut (i.e., 18.9 mm according to Table 1). Accordingly, the number of the nuts that will be cracked simultaneously is 16. The total friction force (F_t) between the drum and nuts (F_t in Equation (12)) was estimated as the value of F multiplied by the total number of almond nuts would be cracked simultaneously (F_t=127×16= 2032 N) and the total compression force (F_{NT}) is equal to 16 × 202.15 = 3234.4 N. Then the value of T (in Equation (12)) is equal to 91.44 N m and the power required (Equation (14)) is equal to 4.1 kW to operate the cracking cylinder at 213 rpm.

Table 1 Physical and mechanical properties of an almond nuts

Property		Min.	Max.	Mean	Stand. Dev.
Length, mm		26.39	30.73	29.05	3.1
Width, mm		17.43	20,41	18.90	6.8
Thickness, mm		14.12	16.88	15.19	5.9
Mass, g		2.8	4.1	3.3	0.28
True density, kg m^{-3}		730	880	790	20
Bulk density, kg m^{-3}		250	480	320	10
Angle of repose, deg.	Empty	33.5	37.3	36.6	1.01
	Filling	34.4	38.1	27.5	2.05
Coefficient of friction	Metal	0.305	0.414	0.352	0.06
	Wood	0.325	0.509	0.465	0.08
	Rubber	0.491	0.625	0.518	0.10
Breaking force, N	Length	322.63	473.60	410.96	8.8
	Width	251.21	312.25	267.13	7.8
	Thickness	162.11	202.15	197.16	4.8

2.1.2 Rotating shaft and bearings

The cracking cylinder is mounted on the rotating shaft; the power is transmitted to the shaft via a pulley mounted on the shaft; two bearings are required to support the shaft as illustrated in Figure 2. The design of a shaft is based on the combined shock, fatigue stresses, and the bending and torsional moments as well.

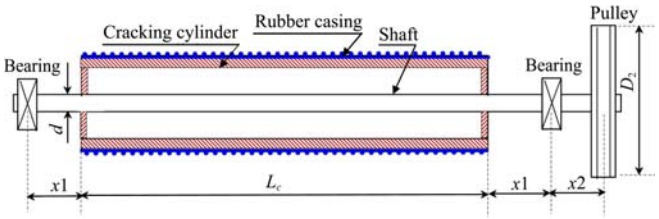

Figure 2 Sectional diagram showing the cracking cylinder and pulley were fixed on the shaft

Hence, the diameter of the shaft was calculated according to (Eric, 1976) as follows:

$$d^3 = \frac{16}{\pi S_s}\sqrt{[K_b M_b]^2 + [K_t M_t]^2} \quad (13)$$

where, d is the shaft diameter (mm); M_b is the resultant bending moment (N m); M_t is the torsional moment (N m); K_b is the combined shock and fatigue factor applied to the bending moment; K_t is the combined shock and fatigue factor applied to the torsional moment, and S_s is the allowable shear stress of the shaft material (N m^{-2}).

Based on the American Society of Mechanical Engineers (ASME) code, and for a gradually applied load to a rotating shaft, the values of K_b and K_t were taken to be 1.5 and 1.0, respectively and the allowable shear stress of the shaft material (S_s) was taken to be 40 MN m^{-2}.

The torsional moment (M_t) is given by (Shigley, 2015) as follows:

$$M_t = \frac{P \times 60}{2\pi N} \quad (14)$$

For the estimated power, P, of 2050 W used to operate the roller at a rotating speed, N, of 213 rpm, value of π is constant (3.14), value of M_t was calculated to be 91.95 N m.

The resultant bending moment, M_b, in Equation (13) is calculated by determining the moments on the shaft due to both the horizontal and vertical loads, and then creating the bending moment diagrams for the shaft to estimate M_b.

2.1.3 Cracking roller

Steel cylinder having an outer diameter of 90 mm, inner diameter of 80 mm, and length (L_c) of 300 mm were used to construct the cracking drum. Two 8-mm thickness steel circular plates were welded to close the sides of the cylinder (Figure 2). In addition, a rubber casing with a high μ value (μ = 0.625) was used to cover the outer surface of the cylinder to increase the friction. The distances, $x1$ and $x2$ in Figure 2 were taken as 100 and 50 mm. The weight of the rubber casing, together with the cylinder (W_c) was estimated to be about 38.7 N.

The angle θ in Figure 1 was estimated from Equation (5) to be 57°. In fact, the drum weight, and the compression and friction forces are uniformly distributed along with the drum length; for the moment analysis, the total of these forces (W_c, F_{NT} and F_t) were taken to act at the middle of the drum.

2.1.4 Pulley

Aluminium pulley was selected, having a diameter (D_2) of 120 mm, and thickness of 40 mm, the static weight of the pulley (W_p) was estimated to be 11.98 N. V-belt was selected according to the ASTM-standard able to transmit 15 kW.

The power transmitted from the pulley of the power source (D_1 in diameter) to the shaft pulley (D_2) through the belt is a function of the belt tension forces (T_1 and T_2) and the pulley speed. The belt tension forces on the pulley were estimated according to (Khurmi and Gupta, 2005) by the following equations.

$$2.3\log\left(\frac{T_1}{T_2}\right)=\mu\theta cosec\beta \quad (15)$$

$$M_t=(T_1-T_2)D_1/2 \quad (16)$$

where, T_1 and T_2 are the tension forces on the tight and loose sides (N), respectively; μ is the friction coefficient between the belt and pulley (μ = 0.25); θ is the warp angle (θ = [180-2α] π /180), radian. The angle α is given by:

$$\alpha=\sin^{-1}\left(\frac{D_1-D_2}{2z}\right) \quad (17)$$

where, z is the distance between the centres of the two pulleys, 60 cm, (between the driven pulley; D_2 and the driving pulley, D_1); In Equation (17), 2 β represents the groove angle of the pulley (32°) and M_t in Equation (16) is the torsional moment (N m).

The transmitted torque by the pulley (M_t) was estimated to be 91.95 N m. From Equation (15) and (16), T_1 and T_2 were estimated and given in Table 2.

Table 2 Values of T_1 and T_2

D_1, mm	D_2, mm	α, degree	θ, radian	(T_1/T_2)	T_1, N	T_2, N	(T_1+T_2), N
120	120	0	3.14	17.3	1626.52	94.02	1720.54
120	211	3.35	3.02312	15.56	1637.75	105.25	1743.01
120	255	6.46	2.91462	14.1	1649.48	116.98	1766.47

The maximum value of (T_1+T_2) was considered in the proposed design. Accordingly, the total vertical load acting at the centre axis of the driven pulley that is equal to ($T_1 + T_2 + W_p$) was estimated to be 1778.45 N.

Finally, the shaft is subjected to the following loads: (i) the vertical components of F_{NT} and F_t acting at the middle of the drum, (ii) the horizontal components of F_{NT} and F_t acting at the middle of the drum, (iii) the vertical load (W_c) acting at the middle of the drum, (iv) the vertical load ($T_1 + T_2 + W_p$) acting at the centre of the driven pulley (D_2), and (v) the reactions at the bearings locations.

In the calculation procedure to determine the shaft diameter (d), the reactions at the bearings locations due to the vertical and horizontal loads were calculated, and the shear forces and the resultant bending moments subjected to the shaft were also calculated. The maximum bending moment on the shaft was found to be 169.6 N m and it will be taken as the M_b in Equation (17). Substituting the values of M_b (169.9 N m) and M_t (91.95 N m) into Equation (17), the resulted value of the shaft diameter (d) should be equal to or higher than 33 mm.

3 Materials and methods

For this study, samples were randomly collected from different farms in Al Bydia, Libya during summer 2015, to be used for the experiments. The moisture contents of the kernel, shell, and hull were 4.5%, 8.8%, and 16.6% d.b., respectively. The physical and mechanical properties of the almond are presented in Table 1. The moisture content measured using an oven dryer at (103°C±2°C) [ASAE S352.2 (ASAE, 1999)].

3.1 Determining the angle of repose

The repose angle (θ, deg.) determined by using an open-ended cylinder of 15 cm diameter and 50 cm height. The cylinder was placed at the centre of a circular plate

having a diameter of 70 cm and filled with nut. The cylinder was raised slowly until it formed a cone on the circular plate. The angle of repose was calculated using the following formula (Karababa, 2006):

$$\theta = \tan^{-1}\left(\frac{2H}{d}\right) \quad (18)$$

where, H is height of the cone (cm).

3.2 Determining the coefficient of static friction

The static coefficient of friction (μ) of almond nut against different materials, namely plywood, galvanized metal and rubber. A device was used for the determination of the friction coefficient as shown in Figure 3 according to Ibrahim (2008). The static coefficient of friction was calculated as follows:

$$\mu = \frac{F_T - F_E}{W} \quad (19)$$

where, F_T is force required to start motion of filled wooden frame (N); F_E is force required to start motion of empty wooden frame (N); W is weight of the object (N).

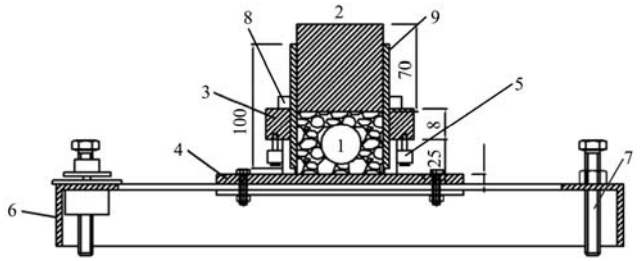

1. Sample 2. Piston 3. Carriage 4. Sliding surface 5. Rolling wheels 6. Base 7. Adjustable screw 8. Adjustable nut 9. Cylinder

Figure 3 The device for measuring the friction force

3.3 Determining the breaking force of almond nuts

The rupture strength was tested to identify the magnitude of force that is required to break the almond nuts. Several trails were conducted with a special press (Bernik and Stajnko, 2009) at the laboratories of Faculty of Engineering, Omar Al Mokhtar University, Libya. Each individual almond was loaded between two parallel jaws and compressed until the nut is ruptured. To determine the required force for nut rupture, nuts were positioned on the front and on the side plane (Figure 4). Five samples, five nuts for each, were selected randomly and the experiment was performed on each sample and the maximum force that breaks the nut was recorded.

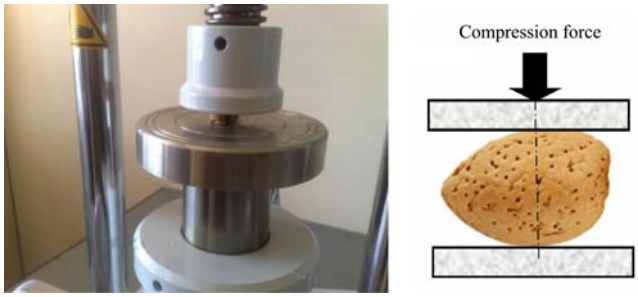

Figure 4 Loading and compressing the nut between two parallel plates

3.4 Fabrication of the cracker

The different parts of the machine were prepared and assembled at the workshop of the College of Engineering, Omar Al-Mokhtar University. A schematic diagram of the machine showing the different parts are illustrated in detail in Figure 5. The Main components of the developed machine were as follows: feeding unit, cracking unit, Separating Unit, electric motor, and power transmission unit.

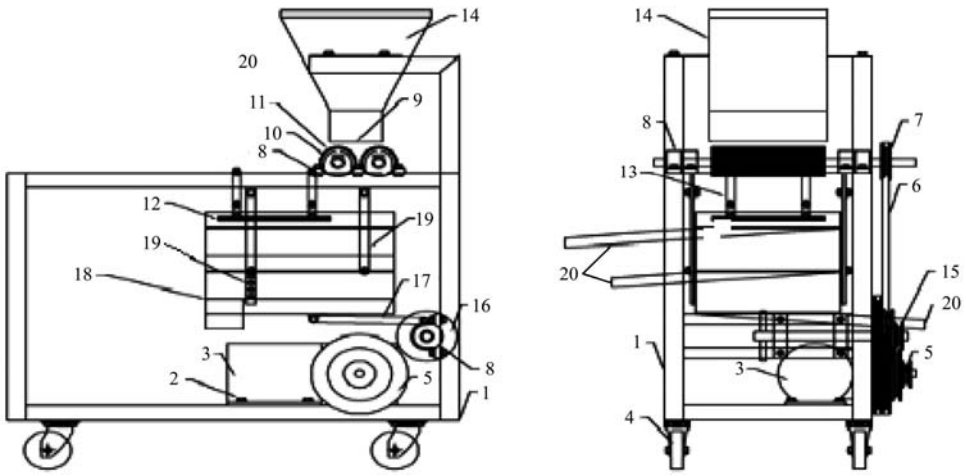

1. Frame 2. Bolts 3. Electric motor 4. Wheel 5. Multi pulleys block 6. V belt 7. Single pulley 8. Bearing housing 9. Gate 10. Roller 11. Roller casing 12. Wooden plate 13. Beam 14. Feed hopper 15. Multi pulleys lock 16. Eccentric crank 17. Connecting rod 18. Oscillating sieves 19. Oscillating rod 20. Collector orifice

Figure 5 Diagrammatic sketch for the developed machine

3.4.1 Feeding unit

A trapezoidal-shape hopper was constructed from steel sheet, 3 mm thickness; it has a square intake upper opening of 400 × 400 mm and outlet base square opening of 200 × 200 mm. The angle between each vertical side of the hopper and the horizontal base is 60° (i.e., the angle of repose of almond nut) to ensure self-feeding and to avoid shattering losses through the feeding unit. The capacity of the hopper was 11.5 kg of almond nuts.

3.4.2 Cracking unit

The cracking unit consists of two rollers with the dimensions of 90 cm in diameter and 300 mm in length for each. The rollers were fabricated using 3 mm thick galvanized steel sheets and covered with a steel mesh grid or a rubber layer of 5 mm thickness (Figure 6). Two steel shafts of 50 mm diameter (according to the theoretical considerations) mounted on a journal bearing at each end of the main farm were utilized to run the rollers (Figure 7). Belt and pulley drive arrangement was set- up to transfer the power from the electric motor (power source) to the main roller. The other roller was free rotating. A stud-nut-spring mechanism contacted to the bearings of the free roller and supported in the frame as shown in Figure 6 to adjust the clearance and the pressure force between the rollers.

Figure 6 Cracking rollers

Figure 7 Stud-nut-spring mechanism

3.4.3 Separating unit

An aggregate of two sieves and flat pan with 60 cm in length and 40 cm in width was fabricated from 3 mm thick steel sheet. The surface area of the upper and lower sieves was covered by a mesh of 24 × 24 mm grids (hols) and 18 × 18 mm, respectively. A decentralized cam was used to convert the rotating motion of the electric motor to reciprocating motion. A wooden plate of 30 cm in length, 40 cm in width and 2 cm thickness was fixed above the sieves. This plate was mounted on the main frame by two iron bars and four springs. The clearance between the wooden plate and sieves was smaller than the nuts dimensions. The separation of the seeds from the solid crust was achieved by the friction between the nuts and the wooden plate that resulted from the reciprocating motion of the sieves.

3.4.4 Electric motor

Electric motor with 3-phase 6 kW at 1440 rpm was used as a power source for the extraction machine. A reduction gearbox was fixed between the motor and the driving shaft to reduce the rotation to 100 rpm.

3.4.5 Power transmission unit

To achieve different roller speeds, different combinations of pulleys were used to transfer the power from the motor to the driving shaft. The diameters of pulleys were determined according to Khurmi and Gupta (2005):

$$N_1 D_1 = N_2 D_2 \quad (20)$$

where, N_1, and D_1 are the rotation (rpm) and diameter of the driving pulley; N_2, and D_2 are the rotation (rpm) and diameter of the driven pulley.

The diameters and rotation of the pulleys corresponding to three different rotation of the roller are illustrated in Table 3.

Table 3 Values of D_1 and D_2 at different roller speeds

Roller speed, m sec^{-1}	Driven Pulley		Driving Pulley	
	N_1, rpm	D_1, mm	N_2, rpm	D_2, mm
0.5	100	120	100	120
0.8	176	120	100	211
1.0	213	120	100	255

3.4.6 Frame and support

A steel frame was made-up from 50 mm × 50 mm steel channel, 3.2 mm thickness, to serve as a skeleton, on

which all the machine components were mounted. The dimensions of the frame are 120 cm in length, 65 cm in width, and 80 cm in height.

4 Performance evaluation

The performance of the constructed machine was investigated at two types of roller casing (rubber and metal mesh), three values of clearance between the rollers (14, 16 and 25 mm) and three different roller speeds (0.5, 0.8 and 1 m s^{-1}). The criteria of the performance evaluation included machine productivity, cracking efficiency, percentage of kernel breakage and specific energy requirements.

The machine productivity (P_m, in kg h^{-1}) was calculated using the following formula:

$$P_m = M/Z \tag{21}$$

where, M The mass of sample before cracking (kg), and Z is the cracking time (h).

The cracking efficiency (CE) is defined as the percentage of the completely cracked nuts to the total nuts that were fed into the hopper. CE was calculated according to the following Equation:

$$CE = \frac{X}{WT} \times 100 \tag{22}$$

where, WT is the total weight of nuts that were fed into the hopper (kg), and X is the weight of the crushed nuts (kg).

The percentage of the kernel breakage is a factor that quantifies the amount of damaged and cracked kernel received from the cracked nuts. Methods of measuring kernel breakage include visual inspection in which the kernel scale appears broken to the naked eye (Srivastava et al., 2006). The percentage of Kernel breakage (PKB, %) was calculated according to the following Equation (23):

$$PKB = \frac{C_d}{C_d + C_u} \tag{23}$$

where, C_d (g) is the cracked and damaged kernel and C_u (g) is the cracked and undamaged kernels.

In order to estimate the power required to operate the machine (RP) and the specific energy consumption (E_s), a digital clamp meter, and voltmeter were used to determine the current and voltage, respectively, supplied to the electric motor during each treatment. The power consumption (P_c, W) was then calculated using the following Equation (24) (Chancellor, 1981):

$$P_c = V \times I \times \cos\theta \tag{24}$$

where, V is the potential voltage difference (220 volt, for single phase); I is the line current (Amp), and $\cos\theta$ is the power factor (0.64).

For each treatment, the specific energy (S_e, kWh kg^{-1}), was calculated by using the following Equation (25):

$$S_e = (P_c/P_m) \tag{25}$$

5 Results and discussion

5.1 Machine productivity

The average values of the machine productivity at different roller speeds as affected by roller clearance for the two roller casings (i.e., rubber and metal mesh) are plotted in Figure 8 (a, b). It could be noticed that increasing the roller speed resulted in increasing the machine productivity at other parameters used in this study. These results may attribute to increasing the nuts flow between the rollers as affected by the roller speed increase that prevents the machine clogging. It can also be observed from Figure 8 (a, b) that increasing the distance between the rollers from 14 to 16 mm tends to increase the productivity at different roller speeds and roller casing. However, increasing the distance to 25 mm resulted in decreasing the machine productivity. The reasons may be due to presence a lot of nuts between rollers as a result of increasing the distance that causes clogging the machine. Figure 8 (a and b) also showed that using rubber casing instead of metal mesh casing caused an increase in the machine productivity at all rollers speeds and distances between rollers. This may be attributed to the fact that the coefficient of a fraction between Almond nuts and rubber is higher than that between Almond nuts and metal mesh, which led to increase the slippage in case of metal mesh.

5.2 Cracking efficiency (*CE*)

The cracking efficiency versus rollers speed and distance between rollers for the two roller casing are demonstrated in Figure 9 (a and b). It can be observed that, at a given rollers clearance and both casing materials, the cracking efficiency decreased with the increase of the roller speed. The cracking efficiency decreased from 68% to 64.65% and from 64.12% to

60.85% as the roller speed increased from 0.5 to 1 m s^{-1} at the rollers clearance of 16 mm for the rubber and metal mesh casing, respectively. These results may be due to increasing the compression time as a result of decreasing the roller speed. At a roller speed of 0.8 m s^{-1} and using metal mesh casing, the cracking efficiency decreased from 69.12% to 38.33% as the rollers clearance increased from 14 to 25 mm. This was attributed to the fact that increase the clearance tends to decrease the compression action.

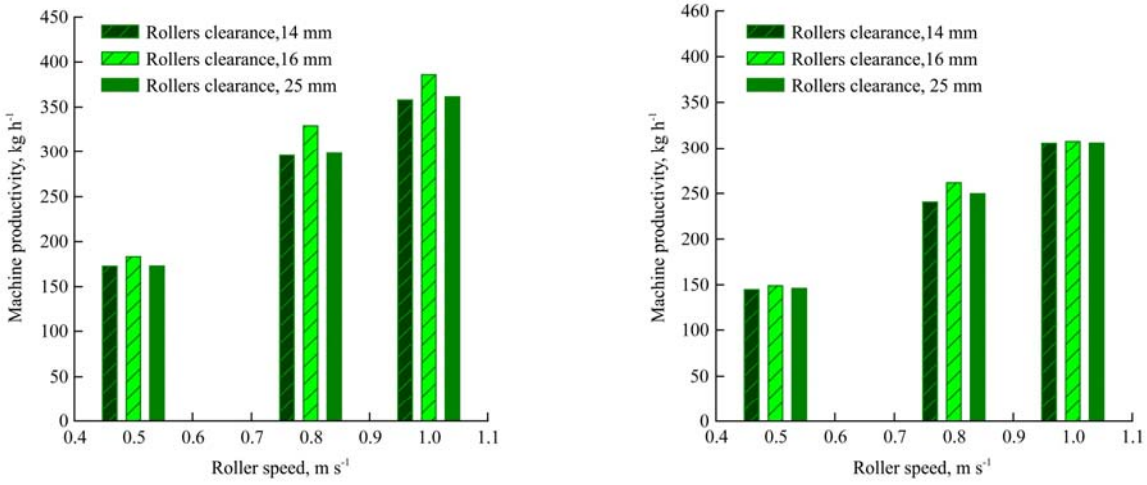

a. Rubber casing b. Metal mesh casing

Figure 8 Effect of roller speed and rollers clearance on the machine productivity

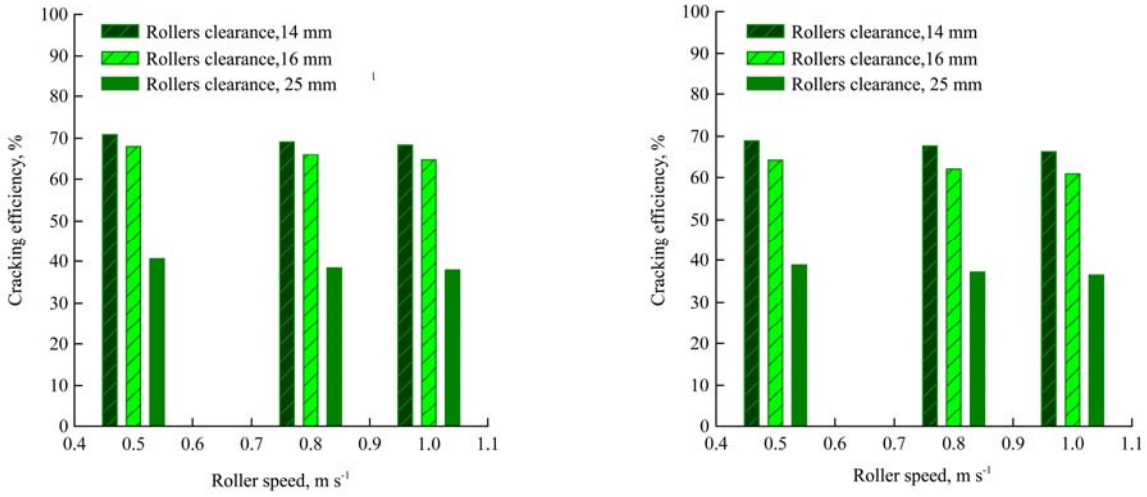

a. Rubber casing b. Metal mesh casing

Figure 9 Effect of roller speed and rollers clearance on the cracking efficiency

5.3 Kernel breakage (*KB*)

Data of the percentage of the kernel breakage as affected by the different operation variables considered in this study is shown in Figure 10 (a and b). At given roller speed and both casing materials, the kernels breakage percentage was observed to decrease with increasing the roller speed. For example, an increase in the roller speed from 0.5 to 1 m s^{-1} caused a drop in the kernel breakage percentage from 13.87% to 12.10% at a rollers clearance of 14 mm when using rubber casing. That was attributed to decrease the impact forces between kernels and rollers by increasing the roller speed. On the other hand, increasing the rollers clearance caused a decrease in the kernel breakage percentage at all levels of roller speed and casing materials used in the study. At a roller speed of 0.5 m s^{-1}, an increase in the percentage of kernel breakage from 11.70% to 13.87% was observed as the roller clearance hiked from 14 to 25 mm for the rubber casing. It can be seen from Figure 9 (a, b) that the kernel breakage in case of metal mesh casing is higher than that in case of the rubber casing.

5.4 Specific energy requirement

The specific energy is defined as being the energy required by the machine to process one Mg of an almond

nut. The average values of the specific energy at different roller speed levels as affected by roller clearance for both casing materials is plotted in Figure 11 (a and b). The general trend in this figure suggested that the required specific energy decreased as the roller speed increased at all levels of roller speeds and both roller casings. Increasing the roller speed from 0.5 to 1 m s^{-1} saved about 57.22% from the required energy led to decrease from 31.75 to 13.58 kWh Mg^{-1} as the roller speed. It could be noticed that the lowest values of the consumed energy were recorded at rollers clearance of 16 mm and rubber casing. However, the highest value of consumed energy was recorded at rollers clearance of 14 mm and metal mesh casing at different roller speeds. These results may be attribute to the increase of the machine productivity at these conditions.

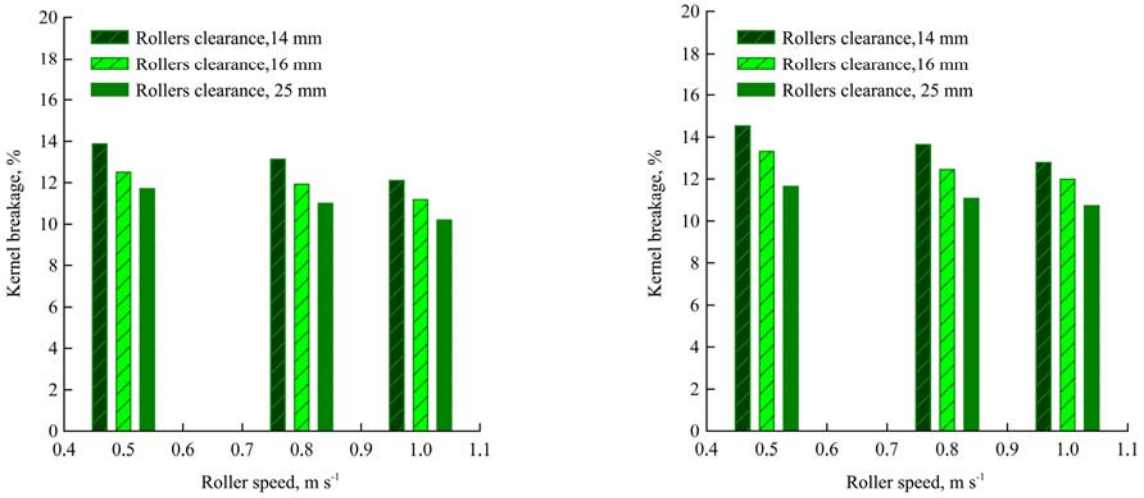

a. Rubber casing b. Metal mesh casing

Figure 10 Effect of roller speed and rollers clearance on the kernel damage

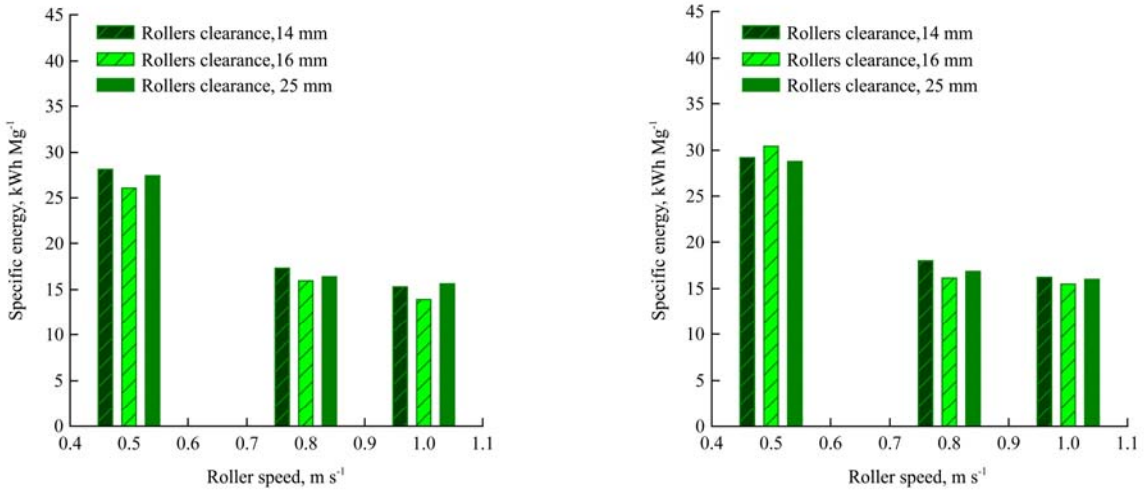

a. Rubber casing b. Metal mesh casing

Figure 11 Effect of roller speed and rollers clearance on the specific energy requirement

5.5 Cracking cost analysis

The cracking cost involved for the developed cracking machine was calculated as follows:

5.5.1 Fixed cost

The machine-related fixed costs included depreciation, interest, taxes, housing and insurance. Assuming a machine life expectancy of five years, an interest rate of 10% and a machine salvage rate of 10% of the machine price (cost) of $ 1000, the annual capital consumption (CC), which included the depreciation and the interest costs, was estimated at 25% of the machine cost (Hunt, 1983). Therefore, the annual CC for the developed machine was estimated at $ 250. With the assumption of 300 operating hours per year, the depreciation and interest costs were calculated at $ 0.833 h^{-1}. The remaining three elements of the fixed costs (interest, taxes and housing)

were, annually, assumed to be 2% of the machine cost (Hunt, 1983), which was calculated at \$ 20 y^{-1}, hence \$ 0.067 h^{-1}. The fixed cost was determined at \$ 0.9 h^{-1}.

5.5.2 Operation (variable) cost

The operational costs included the cost of labor, electric power, repair and maintenance. The labor cost was calculated based on two laborers required to properly operate the machine. This cost was estimated at \$ 10 day^{-1} (8 h day^{-1}), hence the labor cost was calculated at \$ 1.2 h^{-1}. The electric power cost of the machine was determined to be \$ 0.056 h^{-1}. However, the cost of repair and maintenance was estimated at 2% of the machine cost per 100 hours of operation (Hunt, 1983), which was calculated at \$ 0.20 h^{-1}. Therefore, the operation (variable) cost was determined at \$ 1.456 h^{-1}. Then the total machine cost was estimated at \$ 2.356.

The extraction cost (\$ Mg^{-1}) is defined as the machine cost (\$ h^{-1}) divided by the machine productivity (Mg h^{-1}). The extraction cost (\$ Mg^{-1}) at different roller speed levels as affected by roller clearance for the two casing materials are plotted in Figure 12 (a and b). It could be noticed that the lowest values of extraction cost were recorded at roller speed of 1 m s^{-1} and roller clearance of 16 mm, however; the highest values of extraction cost were observed at roller speed of 0.5 m s^{-1} and roller clearance of 14 mm for the two casing materials.

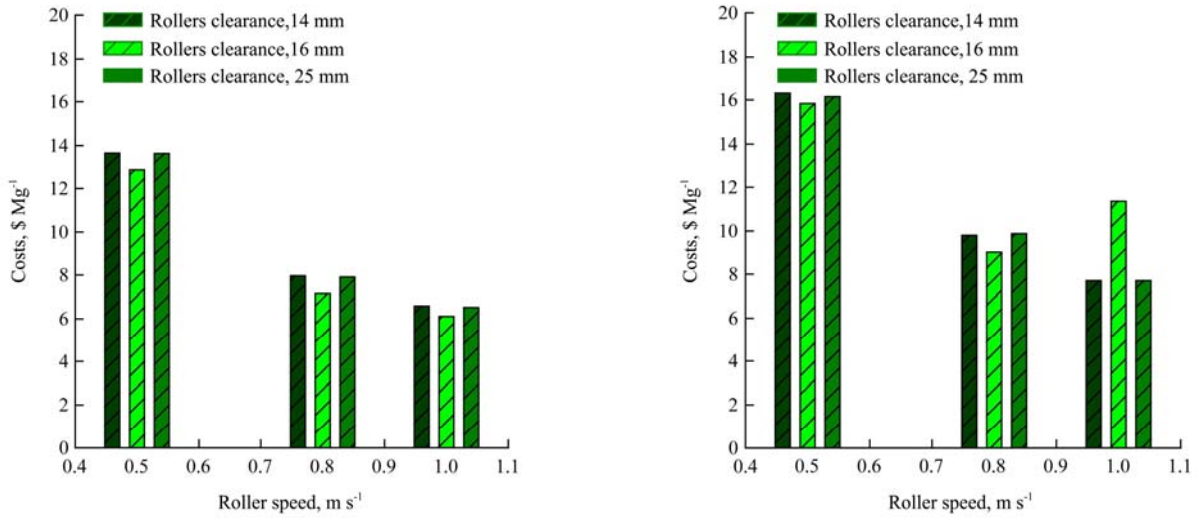

a. Rubber casing b. Metal mesh casing

Figure 12 Effect of roller speed and rollers clearance on the total cost

6 Conclusion

A low-cost almond cracker locally was designed and manufactured. The performance of the developed machine was evaluated at different roller speeds, clearance between the rollers and two rollers casing materials (metal mesh and rubber). The specific conclusions of the study include the following:

The increase of the roller speed from 0.5 to 1.00 m s^{-1} was found to increase the mean value of the machine productivity by 98.8%. However, it caused a decrease in the mean values of the kernel breakage, cracking efficiency, energy requirements and the extraction cost by 11.06, 4.8, 54.59 and 22.56 %, respectively.

At all levels of roller speeds and both casing materials, the clearance between rollers of 16 mm resulted in lowest values of energy requirement 19.56 kW h Mg^{-1}), extraction cost (10.39 \$ Mg^{-1}) and highest values of machine productivity (257.27 kg h^{-1}). On the other hand, the clearance between rollers of 14 mm resulted in the maximum values of cracking efficiency (68.54%).

Cracking efficiency and machine productivity increased by 18.73% and 4.3%, respectively and the kernel breakage, energy requirements and extraction cost decreased by 3.06%, 5.8% and 20.22%, respectively when the rubber casing used instead of the metal mesh casing.

References

Ahmedna, M., W. E. Marshall, A. A. Husseiny, I. Goktepe, and R. M. Rao. 2004. The use of nutshell carbons in drinking water filters for removal of chlorination by-products. *Journal of*

Chemical Technology and Biotechnology, 79(10): 1092–1097.

Altuntas, E., R. Gercekcioglu, and C. Kaya. 2010. Selected mechanical and geometric properties of different almond cultivars. *International Journal of Food Properties*, 13(2): 282–293.

Arnold, R. E. 1964. Experiments with rasp bar threshing drums. I: Some factors affecting performance. *Journal of Agricultural. Engineering Research*, 9(2): 99–131.

ASAE Standards. 1999. ASAE: 567. S352.2 DEC97. Moisture measurement - unground grain and seeds. St. Joseph, Mich.: ASAE.

Aydin, C. 2002. PH-postharvest technology: Physical properties of hazelnuts. *Biosystem Engineering*, 82(3): 297–303.

Aydin, C. 2003. Physical properties of almond nut and kernel. *Journal of Food Engineering*, 60(3): 315−320.

Bernik, R., and D. Stajnko. 2009. A Comparison of morphological and physical characteristics of three different haselnut varieties (*Corylus avellana* L.). *Pomologia Croatica*, 14(4): 221–234.

Borghei, A. M., T. Tavakoli, and J. Khazaei. 2000. Design, construction and testing of walnut cracker. In: Proceedings of European. Agriculture Engineering Conference, Warwick University, England.

Chancellor, W. J. 1981. Substituting information for energy in agricultural. *Transation of the ASAE*, 24(4): 802–807.

Eric, K. G., A. Simons and E. K. Asiam. 2009. The Determination of Some Design Parameters for Palm Nut Crackers, 38(2): 315–327.

Eric, O. 1976. *Machinery's Hand Book*. 20th ed. New York: Industrial Press.

Estevinho, B. N., N. Ratola, A. Alves, and L. Santos. 2006. Pentachlorophenol removal from aqueous matrices by sorption with almond shell residues. *Journal of Hazardous Materials*, 137(2): 1175–1181.

Gbadam, E. K., S. Anthony, and E. K. Asiam. 2009. The determination of some design parameters for palm nut crackers. *Eurpean Journal of Scientific Research*, 38(2): 315–327.

Ghafari, A., G. R. Chegini, J. Khazaei, and K. Vahdati. 2011. Design, construction and performance evaluation of the walnut cracking machine. *International Journal of Nuts and Related Sciences*, 2(1): 11–16.

Guzel, E., P. Ulger, and B. Kayısoglu. 1999. Food Processing Technology of Agricultural Materials. Cukurova Universitesi Ziraat Fakultesi, Genel Yayın No: 145, Adana, Turkey

Hunt, D. 1983. Farm Power and Machinery Management. 8th Ed. Iowa State Univ. Press. Ames, Iowa, USA.

Ibrahim, M. M. 2008. Determination of dynamic coefficient of friction for some materials for feed pellet under different values of pressure and temperature. *Misr Journal of Agriculture Engineering*, 25(4): 1389–1409.

Karababa, E. 2006. Physical properties of popcorn kernels. *Journal of Food Engineering*, 72(1): 100–107.

Khazaei, J. 2008. Characteristics of mechanical strength and water absorption in almond and its kernel. *Cercetări Agronomice în Moldova*, 133(1): 37–51.

Khazaei, J., M. Rasekh, and A. M. Borghei. 2002. Physical and mechanical properties of almond and its kernel related to cracking and peeling. ASAE Paper No. 026153. St. Joseph, Mich.: ASAE.

Khurmi, R. S., and J. K. Gupta. 2005. *Theory of Machines.* New Delhi: Eurasia Publishing house.Koya, O. A. 2006. Palm nut cracking under repeated impact load. *Journal of Applied Sciences*, 6(11): 2471–2475.

Lao, M. T., and S. Jiménez. 2004. Evaluation of almond shell as a culture substrate for ornamental plants. II. Ficus benjamina. *International Journal of Experimental Botany*, 73: 79–84.

Mitchell, R. E., P. A. Campbell, and L. Ma. 2003. Coal and biomass char reactivity. Global Climate and Energy Project, Stanford University., Technical Report. Available at: https://gcep.stanford.edu/pdfs/gcep_brochure.pdf /

Mohsenin, N. N. 1986. *Physical Properties of Plant and Animal Materials*. 2nd ed. New York: Gordon and Breach Science Publishers.

Ogunsina, B. S., O. A. Koya, and O. O. Adeosun. 2008. A table mounted device for cracking dika nut. *CIGR E Journal*, manuscript No.08 011.X.

Ojolo S. J., and B. S. Ogunsina. 2007. Development of a cashew nut cracking device. *CIGR E Journal*, manuscript No. PM 06 030, IX.

Paramount Farms Almonds. 1991. Bakersfield, California: Paramount Farms Company.

Rosengarten, F. 1984. *The Book of Edible Nuts*. New York: Walker Publishing Company, Inc.

Shigley, J. E. 2015. *Mechanical Engineering Design*. S.I (Metric Ed.). New York: Tata, Mcgraw-Hill Publishing Company Limited.

Srivastava, A. K., C. E. Goering, R. P. Rohrbach and D. R. Buckmaster. 2006. Engineering principles of agricultural machines. ASAE Paper No. 631.3/S774. St. Joseph, Mich.: ASAE.

Wang, J. K. 1963.The design of a ground berry-husking machine. *Transaction of the ASAE*, 6(4): 311–312.